Exact surface wave spectrum of a dilute quantum liquid

Peter V. Pikhitsa[1] and Uwe R. Fischer[2]

[1]*Department of Mechanical and Aerospace Engineering, Seoul National University, 08826 Seoul, Korea*
[2]*Center for Theoretical Physics, Department of Physics and Astronomy, Seoul National University, 08826 Seoul, Korea*
(Dated: December 20, 2018)

We consider a dilute gas of bosons with repulsive contact interactions, described on the mean-field level by the Gross-Pitaevskii equation, and confined by an impenetrable wall (either rigid or flexible). We solve the Bogoliubov-de Gennes equations for excitations on top of the Bose-Einstein condensate analytically, by using matrix-valued hypergeometric functions. This leads to the exact spectrum of gapless Bogoliubov excitations localized near the boundary, which form an excitation branch separated from the bulk excitation spectrum of the condensate by a finite binding energy. Here, either the surface of liquid helium, for which mean-field theory represents an approximation, may constitute the boundary, or alternatively the surface of a box-trapped dilute Bose-Einstein-condensed gas, provided that the walls of the box can be made either effectively rigid or flexible. The dispersion relation for the surface excitations gives for small wavenumbers k a ripplon mode with fractional dispersion relation for a flexible wall, and a phonon mode (linear dispersion) for a rigid wall. For both modes we provide, for the first time, the exact dispersion relations of the dilute quantum liquid for all k along the surface, extending to $k \to \infty$. For a rigid wall with zero boundary conditions we provide an exact algebraic equation for the energy spectrum, while for the ripplon mode the energy spectrum can be obtained by a hypergeometric series, which even to lowest order is close to the one obtained from a numerical solution. The small wavelength excitations are shown to be bound to the surface with a maximal *universal* binding energy $\Delta \simeq 0.158 \, mc^2$, identical for both excitation branches, where m is mass of bosons and c bulk speed of sound.

I. INTRODUCTION

Initially the Gross-Pitaevskii equation (GPE) was intended as a model to describe structures and excitations in superfluid helium.[1,2] Being a nonlinear Schrödinger equation, it was however recognized later on that it possesses a variety of applications for various nonlinear processes in condensed matter such as bright and dark solitons in Bose-Einstein condensates (BECs, for which the GPE is accurate on the mean-field level)[3] and nonlinear optics,[4] as well as finite amplitude waves on the surface of a liquid.[5] Excitations on top of the mean-field ground state representing the Bose-Einstein condensate, known as Bogoliubov excitations,[6] are described by the eigenmodes of the matrix Bogoliubov-de Gennes equations (BdGE). The associated quanta of the perturbation field have become the archetype of quasiparticle excitations in superconductivity[7–9] and the theory of dilute quantum gases,[10] e.g., for the formulation of the propagation of quantum fields on effective curved spacetimes.[11] The ubiquitous nature of the BdGE makes rigorous analytical solutions highly desirable, but very few, and only in limiting cases, have been obtained.

Domain wall solutions of the GPE such as 2D dark solitons are known to be unstable except for those in the presence of a hard wall. Yet even the case of the hard wall deserves investigation inasmuch it is connected with the generic topic of edge excitations in topological phases. In particular, the situation bears some resemblance to two-band models with Majorana bound states that arise as solutions to three dimensional BdG theories. The gapless modes that propagate along a physical boundary, while they are exponentially decaying away from the physical boundary, are gapless boundary modes or edge states.[12]

Examples for surface excitations in confined BECs comprise, for example, superfluid ^{4}He (helium II) confined in pores,[13] self-bound condensates at the low-density surface of superfluid helium,[14] as well as surface states of a dilute BEC trapped in an external potential[15], or in media with a defocusing nonlinearity.[16] These surface excitations are of fundamental interest since they reveal the role of quantum effects of excitations (i.e., not existing on the classical level) in restricted geometries. One way to obtain surface excitations of a BEC was considered in the work by Anglin,[15] which treats the surface excitation of a stable BEC by semianalytical means in the presence of an external linear trapping potential.

Considering the extreme boundary condition of the hard wall for the surface of a trapped BEC, the stability of surface bound states was proven in[16], by imposing the boundary condition of zero wavefunction at the wall. Such potentials much steeper than harmonic were prepared by using laser sheets to trap bulk dilute quantum gases (for example, in[17]). An inhomogeneous stationary solution of the GPE (the "domain wall") which coincides with the half of the dark soliton (kink) at rest,[3] may have as one of its physical realizations a hard wall[16] where localized Bogoliubov excitations were proposed to exist.[18] However, the full analytical solution for the corresponding surface-bound excitations has not been found before. At large wavelengths, one class of these excitations represents a surface phonon and the other a ripplon. Our approach is inherently quantum, as it operates near the node plane of the domain wall-soliton, and is hence based on an inherently nonclassical (vector-valued) wavefunction, and is not restricted to large wavelengths, where

the (essentially quantum) kinetic terms are small. We note that the existence of a short-wavelength surface excitation (a "surface roton") was previously conjectured,[19] but its possible connection to capillary waves was then stated as being doubtful. We will see below that for both classes of excitations, starting either from surface phonon or ripplon at large wavelengths, a small-wavelength surface excitation with a *universal* binding energy, which is identical for both branches, can exist.

The hard wall boundary condition may also approximate the sharpness of a self-bound potential at a free surface of liquid helium, which was proven to be composed of a nearly pure condensate of dilute bosonic gas that satisfies the GPE.[14] This is because one may consider the free kink wall with profile $\psi_0 = \tanh(x)$ as a model for a free surface into the bulk of the liquid ($x \geq 0$), demanding only the topological stability of such a solution for which its nodal surface undergoes weak flexural oscillations. Then the position of the hard wall is flexible (like an impenetrable membrane on the surface of helium II) and imitates the free surface of the liquid. The liquid surface of helium II is under these provisos equivalent to a hard wall container.

Here we consider the problem of localized gapless excitation modes by finding analytical solutions of a matrix Schrödinger equation which we show to be equivalent to the BdGE.[16,18,20,21] While recently, Ref.[22] obtained such an analytical solution in the presence of a domain wall, it is restricted to large wavelengths, and furthermore faces the difficulty of extrapolation to the case of an infinite-size surface. The binding energy of localized excitations is a primary quantity of interest. Recent experiments that prove the common physical origin of the Landau description of a superfluid and the BEC description[23] support the view that the binding energy is relevant to the superfluid. Furthermore, neutron scattering experiments in helium II[24] reveal a surface branch of the excitation spectrum that directly gives the binding energy. Remarkably, we show that the spectrum of surface excitations can be calculated analytically for *any* wavevector k, reproducing the numerical results and with the analytical results obtained for limiting cases $k \to 0$ and $k \to \infty$. We have solved the BdGE for the case of the domain wall (see Eqs. (4.16-4.19) in[22]). The limit of $k \to \infty$, which in the bulk BEC results in the energy spectrum $\varepsilon = \hbar^2 k^2 / 2m + \mu$ where m is the mass of the boson and $\mu = gn_0$ is the chemical potential while g and n_0 are the coupling constant and the BEC particle density, respectively, then leads to $\varepsilon = \hbar^2 k^2 / 2m + \mu - \Delta$.

II. BOGOLIUBOV-DE GENNES EQUATIONS

A. Basic setup

The GPE of a scalar quantum gas can be written as:[25]

$$i\hbar \frac{\partial \psi}{\partial t} = -\frac{\hbar^2}{2m} \nabla^2 \psi + gn_0(|\psi|^2 - 1)\psi. \qquad (1)$$

We introduce dimensionless quantities by measuring distances in the units of the healing length $\xi = \hbar/mc$ and energies in units of the "rest mass energy" $gn_0 = mc^2$ where $c = \sqrt{gn_0/m}$ is the sound velocity. The stationary equation (1) for the kink with the node at the position $x = 0$ gives the wavefunction $\psi_0 = \tanh(x)$ of the soliton. We will impose perturbations on this solution to investigate its Bogoliubov excitations by representing ψ of Eq. (1) as a sum of plane waves:[2] $\psi = \psi_0(x) + \vartheta(\vec{r}, t)$ with $\vartheta(\vec{r}, t) = a_{\omega,\vec{k}}(x)\exp(i\vec{k}\cdot\vec{\varrho} - i\omega t) + b^*_{\omega,\vec{k}}(x)\exp(-i\vec{k}\cdot\vec{\varrho} + i\omega t)$, where $\vec{r} = (x, \vec{\varrho})$, $\vec{\varrho}$ lies in the plane orthogonal to the x direction (we consider the situation that all functions decay exponentially with increasingly larger positive x), $\vec{k}$ is the wave vector along this plane and * denotes complex conjugation. We will suppress the indices and simplify the notation by using a and b instead of $a_{\omega,\vec{k}}(x)$ and $b_{\omega,\vec{k}}(x)$. Introducing the functions $\psi_1 = a + b$ and $\psi_2 = a - b$, after linearizing Eq. (1) we get a pair of coupled Schrödinger equations:[18]

$$-\frac{1}{2}\frac{d^2}{dx^2}\psi_1 + (3\psi_0^2 - 1 + \kappa^2)\psi_1 = \varepsilon\psi_2, \qquad (2)$$

$$-\frac{1}{2}\frac{d^2}{dx^2}\psi_2 + (\psi_0^2 - 1 + \kappa^2)\psi_2 = \varepsilon\psi_1, \qquad (3)$$

where $\kappa = \xi|\vec{k}|/\sqrt{2}$ and $\varepsilon = \hbar\omega/(mc^2)$. This pair of equations is identical to the corresponding Bogoliubov-de Gennes equations (see[20,26]) if one rewrites them for the functions a and b. To the best of our knowledge, Eqs. (2) and (3) have never been solved exactly before for arbitrary non-zero κ and ε. We find a formal general solution for these equations and illustrate its viability by obtaining the rigorous solution of the spectrum of localized phonons.

The spectrum of bulk excitations can be easily found from (2) and (3) when neglecting the derivative terms far from the boundary $x = 0$ to obtain the well-known Bogoliubov spectrum $\varepsilon_B = \kappa\sqrt{2 + \kappa^2}$. For $\kappa \to 0$, it gives the bulk phonon dispersion $\varepsilon_B \simeq \sqrt{2}\kappa + \kappa^3/(2\sqrt{2})$ and for $\kappa \to \infty$ $\varepsilon_B \simeq \kappa^2 + 1$ which is a free boson plus the chemical potential. The localized excitations to be derived, by definition, have an energy spectrum lying lower than the bulk one.

B. Supersymmetry at exceptional point

We first remark that at the exceptional point of symmetry $\varepsilon = 0$ and $\kappa = 0$, Eqs. (2) and (3) are the parts

of a supersymmetric Hamiltonian with zero ground state energy. Indeed, on introducing the matrix operator

$$\hat{A} = \begin{pmatrix} -\frac{1}{\sqrt{2}}\frac{d}{dx} - \sqrt{2}\psi_0 & 0 \\ 0 & -\frac{1}{\sqrt{2}}\frac{d}{dx} + \frac{1}{\sqrt{2}}\frac{1-\psi_0^2}{\psi_0} \end{pmatrix} \quad (4)$$

so that the l.h.s. of Eqs. (2) and (3) takes the form of a matrix Hamiltonian

$$\hat{H}_- = \hat{A}^\dagger \hat{A} = \begin{pmatrix} -\frac{1}{2}\frac{d^2}{dx^2} + 3\psi_0^2 - 1 & 0 \\ 0 & -\frac{1}{2}\frac{d^2}{dx^2} + \psi_0^2 - 1 \end{pmatrix}$$
$$(5)$$

with its partner Hamiltonian

$$\hat{H}_+ = \hat{A}\hat{A}^\dagger = \begin{pmatrix} -\frac{1}{2}\frac{d^2}{dx^2} + \psi_0^2 + 1 & 0 \\ 0 & -\frac{1}{2}\frac{d^2}{dx^2} + \frac{1-\psi_0^2}{\psi_0^2} \end{pmatrix}(6)$$

to produce a supersymmetric (SUSY) Hamiltonian

$$\hat{H}_{\text{SUSY}} = \begin{pmatrix} \hat{H}_- & 0 \\ 0 & \hat{H}_+ \end{pmatrix} \quad (7)$$

that may canonically be expressed through the supercharges

$$\hat{Q} = \begin{pmatrix} 0 & 0 \\ \hat{A} & 0 \end{pmatrix}, \hat{Q}^\dagger = \begin{pmatrix} 0 & \hat{A}^\dagger \\ 0 & 0 \end{pmatrix} \quad (8)$$

as an anticommutator

$$\hat{H}_{\text{SUSY}} = \{Q, Q^\dagger\}; \hat{Q}^2 = 0, (\hat{Q}^\dagger)^2 = 0. \quad (9)$$

The supersymmetry is explicitly broken when either ε or κ (or both) are not zero which eventually, as we will discuss in detail below, leads to splitting the degenerate zero ground state into two gapless excitations (a "light" one with $\varepsilon \propto \kappa$ and a "heavy" one with $\varepsilon \propto \kappa^{3/2}$),[18] both bound to the wall.

C. Boundary conditions

The boundary conditions for ψ_1 and ψ_2 in (2) and (3) form two distinct classes. At the node of the kink $\psi = 0$, that is both Im $\psi = 0$ and Re $\psi = 0$, and therefore also $\psi_2 = 0$ and $\psi_1 = 0$. However, for ψ_1, an additional possibility exists. Indeed, for $\kappa = 0$ and $\varepsilon = 0$, Eqs. (2) and (3) have the solutions $\psi_1^0 = 1 - \psi_0^2$ and $\psi_2^0 = \psi_0$, the first of which is the so-called "zero mode",[18,26] which leads to Goldstone gapless modes (ripplons and phonons) when the SUSY is broken. This corresponds to a translation of the kink ψ_0 as a whole along x, resulting in the derivative of the kink ψ_0 as follows: $\psi_0(x+\delta x) \simeq \psi_0(x) + \psi_0' \delta x$. Thus the condition Re $\psi = 0$ turns into $\psi_0' \delta x(\vec{\varrho}, t) + \text{Re } \vartheta(\vec{r}, t) = 0$ which determines the shape of the loci of nodes $\delta x(\vec{\varrho}, t)$ (the shape of the surface). The derivative of such a mode with respect to x is zero at $x = 0$. The mode with the mixed boundary

conditions $\frac{d}{dx}\psi_1 \mid_{x=0} = 0$ and $\psi_2 \mid_{x=0} = 0$ allows the "rippling" of the soliton and is thus called *ripplon* mode.[18] As we shall see below, its energy spectrum at low κ coincides with the one for a classical capillary wave. The mode with zero boundary conditions $\psi_1 \mid_{x=0} = 0$ and $\psi_2 \mid_{x=0} = 0$, which correspond to a flat boundary hard wall will be called *surface phonon* mode (with a spectrum starting linear).[18] Finally, the very condition of a well-defined wall excludes the possible solution $x\psi_0 - 1$[21] of Eq. (3) at $\kappa = 0$, $\varepsilon = 0$ which could lead to the so-called snake instability[16,21,27], and which does not satisfy zero boundary conditions.

III. ASYMPTOTIC SOLUTIONS

We first derive the large and small wavelength solutions of the BdGE, noting also that solely the large wavelength case has been considered before.[18,22]

A. Large wavelengths

First consider the case of $\kappa \to 0$. For the ripplon spectrum we make an ansatz for $\psi_{1,2}$ in the form of series in ε: $\psi_1 \simeq \psi_1^0 + \varepsilon\psi_1^1 + \mathcal{O}(\varepsilon^2)$ and $\psi_2 \simeq \psi_2^0 + \varepsilon\psi_2^1 + \mathcal{O}(\varepsilon^2)$. A zeroth-order approximation is the solution of the homogeneous equations Eqs. (2) and (3) with $\varepsilon = 0$. The solutions can be found for any κ (this can be verified by direct substitution):

$$\psi_1^0 = A\exp(-\alpha_1 x)\left(\frac{\alpha_1^2 - 1}{3} + \alpha_1\psi_0 + \psi_0^2\right), \quad (10)$$

$$\psi_2^0 = B\exp(-\alpha_2 x)(\psi_0 + \alpha_2), \quad (11)$$

where $\alpha_1 = \sqrt{2}\sqrt{2+\kappa^2}$ and $\alpha_2 = \sqrt{2}\kappa$. To determine ψ_1^1 and ψ_2^1 we have to solve the inhomogeneous equations that follow from Eqs. (2), (3) where $\kappa = 0$:

$$-\frac{1}{2}\frac{d^2}{dx^2}\psi_1^1 + (3\psi_0^2 - 1)\psi_1^1 = B\psi_0, \quad (12)$$

$$-\frac{1}{2}\frac{d^2}{dx^2}\psi_2^1 + (\psi_0^2 - 1)\psi_2^1 = A(1 - \psi_0^2). \quad (13)$$

With the help of the Green functions of the homogeneous equations the inhomogeneous solutions are found as:

$$\psi_1^1 = B\frac{1}{2}\left\{\psi_0 + x(1 - \psi_0^2)\right\}, \quad (14)$$

$$\psi_2^1 = -A. \quad (15)$$

Finally, the derivative with respect to x of ψ_1 at $x = 0$ is found from Eqs. (10), (14) to be $\psi_1' = A\alpha_1(2 - \alpha_1)(2 + \alpha_1)/3 + \varepsilon B$, which according to the mixed boundary conditions should be zero together with $\psi_2 = -A\varepsilon + B\alpha_2$, as it follows from Eqs. (11) and (15). The zero determinant
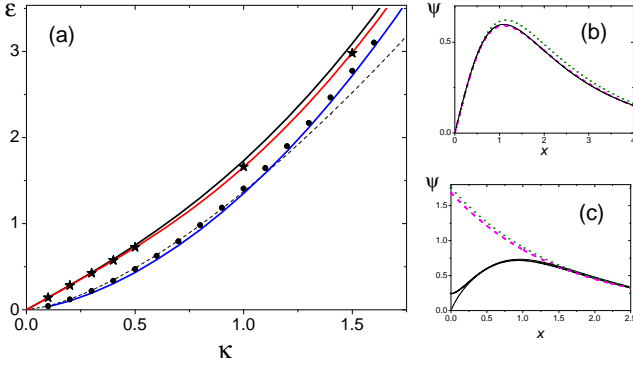
FIG. 1. The dimensionless spectra of the elementary excitations vs the dimensionless wavenumber and wavefunctions. (a) The thick solid line is the Bogoliubov bulk excitation spectrum and the dashed line is the capillary wave spectrum (17). The circles mark the spectrum of the ripplon calculated by numerically solving Eqs. (2) and (3), and the blue line shows the first approximation of the exact solution of Eq. (42). Finally, the stars mark the numerical spectrum of the surface phonon, and the red line is the exact solution (37). (b) The numerical wavefunctions of the surface phonon at $\kappa = 3.5$ are shown with dashed (ψ_1) and dotted (ψ_2) lines together with ψ_∞ (solid line) which they approach at large x. (c) The numerical wavefunctions of the ripplon mode at $\kappa = 5$. It is seen that ψ_1 (thick solid line) lies very close to ψ_2 except the coordinate origin where ψ_1 has zero derivative. The dashed purple and dotted green lines show the asymptotic behavior $\propto \exp(-\alpha_2 x)$ for $\psi_{1,2}$.

with respect to A and B

$$\det \begin{pmatrix} \alpha_1(2-\alpha_1)(2+\alpha_1)/3 & \varepsilon \\ -\varepsilon & \alpha_2 \end{pmatrix} = 0 \qquad (16)$$

gives the ripplon spectrum taking into account that $\alpha_1 \simeq 2 + \kappa^2/2$ for $\kappa \to 0$ and retaining only the lowest power of κ, we obtain the fractional dispersion

$$\varepsilon = \sqrt{\frac{4\sqrt{2}}{3}} \kappa^{3/2}. \qquad (17)$$

The spectrum (17) is shown in Fig. 1. Note that the localization of the ripplon at low κ is governed by $\alpha_2 = \sqrt{2}\kappa$. The spectrum (17) coincides with the well-known expression for the frequency of capillary waves (in the deep water limit), which reads in dimensional form $\varepsilon = \hbar\sqrt{\sigma/mn_0}\ k^{3/2}$ where $\sigma = \frac{2}{3}\hbar c n_0$ is the surface energy density of the stationary soliton ψ_0.[25] We note that σ is exactly the half of the energy of the dark soliton at rest [see Eq. (5.59) in[3]].

The zero boundary conditions lead to surface phonons for $\kappa \to 0$ (cf.[18]) and below we obtain the whole surface phonon spectrum analytically. We here only mention in connection to the above discussion that α_2 for phonons at low κ is proportional to κ^2, indicating a much weaker localization as compared to the ripplons.

B. Small wavelengths

When $\kappa \to \infty$, we introduce the function χ and constant Δ so that $\psi_1 = \psi_2 + \chi/k^2$, $\psi_2 = \psi_\infty$ and $\epsilon = \kappa\sqrt{\kappa^2+2} - \Delta \asymp \kappa^2 + 1 - \Delta$. Then Eqs. (2), (3) turn into

$$-\frac{1}{2}\frac{d^2}{dx^2}\psi_\infty + (3\psi_0^2 - 2 + \Delta)\psi_\infty = -\chi, \qquad (18)$$

$$-\frac{1}{2}\frac{d^2}{dx^2}\psi_\infty + (\psi_0^2 - 2 + \Delta)\psi_\infty = \chi, \qquad (19)$$

with $\chi = -\psi_0^2\psi_\infty$, which after adding and subtracting both equations leads to

$$\psi_\infty = (1 - \psi_0^2)^{\alpha_\infty/2}$$
$$\times\ _2F_1\left(\alpha_\infty - s, \alpha_\infty + s + 1, \alpha_\infty + 1, \frac{1-\psi_0}{2}\right), \quad (20)$$

where the hypergeometric function contains $\alpha_\infty = \sqrt{2\Delta}$ and $s = (\sqrt{17}-1)/2$ is one of the solutions of the equation $s(s+1) = 4$ (see[28]). The second solution leads to the same result. The boundary condition $\psi_2 = 0$ at $x = 0$ imposes the following identity

$$_2F_1\left(\alpha_\infty - s, \alpha_\infty + s + 1, \alpha_\infty + 1, \frac{1}{2}\right) =$$
$$\frac{\Gamma(\frac{1}{2})\Gamma(\alpha_\infty + 1)}{\Gamma(\frac{1}{2}[1 + \alpha_\infty - s])\Gamma(\frac{1}{2}[2 + \alpha_\infty + s])} = 0. \quad (21)$$

which demands (for fixed s) $1 + \alpha_\infty - s = 0$ in order to have the infinity in the denominator from the corresponding gamma function, and therefore $\alpha_\infty = (\sqrt{17} - 3)/2 \simeq 0.562$ while $\Delta = \alpha_\infty^2/2 \simeq 0.158$. Finally, the hypergeometric function in (20) reduces to ψ_0 so that $\psi_\infty = \psi_0(1 - \psi_0^2)^{\alpha_\infty/2} = \tanh(x)/\cosh(x)^{\alpha_\infty}$ (see Fig.1 (b)) and $\chi = -\psi_0^3(1 - \psi_0^2)^{\alpha_\infty/2}$. Therefore, both ψ_2 and ψ_1 satisfy the zero boundary conditions. Analogously, one can show[29] that the function ψ_∞ is also the limiting function for large κ for the mixed boundary conditions, so that the difference between the functions appears only in close proximity to the boundary $x = 0$, at a typical distance $1/\kappa$ [see Fig.1 (c); ψ_1 deviates from ψ_2 and hits the ψ axis with zero derivative]. Thus the binding energy of the excitation localized near the surface behaves universally (depending only on the bulk parameters) as well as its wavefunction does. In dimensional units, this binding energy is $0.158\,mc^2 \simeq 4\,\mathrm{K}$.

IV. EXACT SOLUTION OF THE FULL BDGE

We now aim at finding the exact solution of Eqs. (2), (3) at *arbitrary* adimensionalized momentum κ. To do so, let us transform these equations into a single matrix hypergeometric equation, where we employ the fact that matrix generalizations of both hypergeometric function

and gamma function were previously shown to be mathematically viable tools.[30,31] Introducing

$$z = \frac{1 - \psi_0}{2}, \qquad \psi_{1,2} = (1 - \psi_0^2)^{\alpha/2} \phi_{1,2}, \qquad (22)$$

we rewrite Eqs. (2), (3) into

$$z(1 - z)\frac{d^2\phi_1}{dz^2} + \{\alpha + 1 - 2(\alpha + 1)z\}\frac{d\phi_1}{dz}$$
$$+ \{6 - \alpha(\alpha + 1)\}\phi_1 + \frac{1}{2z(1 - z)}\left(\frac{\alpha^2}{2} - 2 - \kappa^2\right)\phi_1$$
$$= \varepsilon\frac{\phi_2}{2z(1 - z)},$$

$$z(1 - z)\frac{d^2\phi_2}{dz^2} + \{\alpha + 1 - 2(\alpha + 1)z\}\frac{d\phi_2}{dz}$$
$$+ \{2 - \alpha(\alpha + 1)\}\phi_2 + \frac{1}{2z(1 - z)}\left(\frac{\alpha^2}{2} - \kappa^2\right)\phi_2$$
$$= \varepsilon\frac{\phi_1}{2z(1 - z)}. \qquad (23)$$

To turn (23) into a matrix hypergeometric equation, we introduce the vector-function $\hat{\Phi}$, the unity $\hat{1}$, the matrix $\hat{\alpha}$, and matrices $\hat{a}, \hat{b}, \hat{c}$ derived from it, as follows

$$\hat{\Phi} = \begin{pmatrix} \phi_1 \\ \phi_2 \end{pmatrix}, \qquad (24)$$

$$\hat{\alpha}^2 = 2\begin{pmatrix} 2 + \kappa^2 & \varepsilon, \\ \varepsilon & \kappa^2 \end{pmatrix}, \qquad (25)$$

$$\hat{c} = \hat{\alpha} + \hat{1}, \qquad (26)$$

$$\hat{1} + \hat{a} + \hat{b} = 2(\hat{\alpha} + \hat{1}), \qquad (27)$$

$$-\hat{a}\hat{b} = \begin{pmatrix} 6 & 0 \\ 0 & 2 \end{pmatrix} - \hat{\alpha}^2 - \hat{\alpha}. \qquad (28)$$

Taking the square root of the matrix $\hat{\alpha}^2$ gives, choosing the positive sign,

$$\hat{\alpha} = 2\begin{pmatrix} r & l \\ l & p \end{pmatrix}, \qquad (29)$$

where $r = \sqrt{1 + \kappa^2/2 - l^2}$, $p = \sqrt{\kappa^2/2 - l^2}$, and $l = \varepsilon\sqrt{\kappa^2 + 1 - (\kappa^2(\kappa^2 + 2) - \varepsilon^2)^{1/2}}/(2\sqrt{\varepsilon^2 + 1})$. The positive eigenvalues of the matrix $\hat{\alpha}$ are

$$\alpha_{1,2} = \sqrt{2}\sqrt{1 + k^2 \pm \sqrt{\varepsilon^2 + 1}} \qquad (30)$$

and $\exp(-\alpha_2 x)$ determines the asymptotic decay of ψ_1 and ψ_2 as $x \to \infty$. After introducing the matrices, Eq. (23) becomes

$$z(1 - z)\hat{\Phi}'' + (\hat{c} - (\hat{1} + \hat{a} + \hat{b})z)\hat{\Phi}' - \hat{a}\hat{b}\hat{\Phi} = 0, \quad (31)$$

where primes mean differentiation with respect to z.

Equation (31) has a formal solution as the matrix-valued hypergeometric function[30]

$$_2F_1(a, b, c, z) = \sum_{n \geq 0} \frac{z^n}{n!}(\hat{a}, \hat{b}, \hat{c})_n, \qquad (32)$$

where $(\hat{a}, \hat{b}, \hat{c})_0 = \hat{1}$, and higher matrix coefficients are

$$(\hat{a}, \hat{b}, \hat{c})_{m+1} = (\hat{c} + m\hat{1})^{-1}(\hat{a} + m\hat{1})(\hat{b} + m\hat{1})$$
$$\times (\hat{c} + m\hat{1} - \hat{1})^{-1}(\hat{a} + m\hat{1} - \hat{1})(\hat{b} + m\hat{1} - \hat{1}) \ldots \hat{c}^{-1}\hat{a}\hat{b}. \qquad (33)$$

A. Surface phonons

We use the formal solution (32) to obtain the spectrum of the surface phonon localized near the soliton–domain wall. The boundary condition at $x = 0$ (that is at $z = 1/2$) will be fulfilled when $\hat{\Phi} = 0$. The hypergeometric function at $z = 1/2$ can be expressed through the matrix gamma function[31] [because $\hat{c} = (\hat{1} + \hat{a} + \hat{b})/2$, see Eq.(27)], so that

$$_2F_1\left(\hat{a}, \hat{b}, \hat{c}, \frac{1}{2}\right) = \frac{\Gamma(\frac{1}{2})\Gamma(\hat{c})}{\Gamma\left(\frac{1}{2}[\hat{1} + \hat{a}]\right)\Gamma\left(\frac{1}{2}[\hat{1} + \hat{b}]\right)}. \qquad (34)$$

Then the condition of zero $\hat{\Phi}$ means that the matrix (34) has a zero eigenvalue, that is the determinant of (34) should be zero. In turn, matrix gamma functions can be represented as the products of matrices[31]

$$\Gamma(\hat{M}) = \lim_{n \to \infty}(n - 1)!n^{\hat{M}}[\hat{M}(\hat{M} + \hat{1})\ldots(\hat{M} + n\hat{1})]^{-1}. \qquad (35)$$

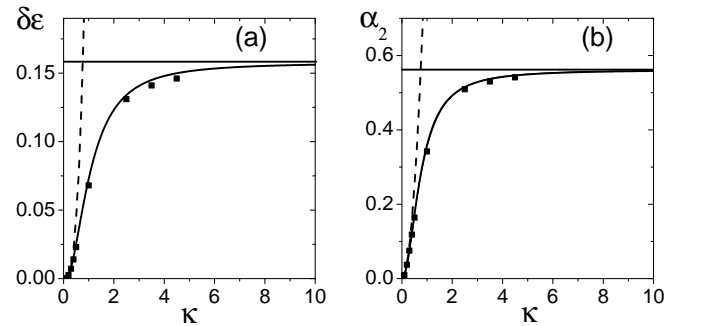Therefore, the determinant of (34) being zero is ex-

FIG. 2. *Surface phonon:* (a) Binding energy vs wavenumber. The solid line is the result of the exact solution given by Eq. (37). The squares show the results of the numerical solution of Eqs. (2) and (3) with zero boundary conditions. The horizontal line is at Δ; the dashed line is $\kappa^3/(2\sqrt{2})$ from the small κ behavior. (b) Solid line: Exact solution for α_2 given by Eqs. (37) and (30). The horizontal line is at α_∞; the dashed line is κ^2.

pressed by either the determinant of $\hat{1}+\hat{a}$ or that of $\hat{1}+\hat{b}$ being infinity. One can prove that the determinant of either of them gives the same spectrum. However an analytical solution for the matrix equations (27), (28) for $\hat{a}$ and $\hat{b}$ is difficult. To obtain analytical results we will instead utilize the product $\hat{P} = ((\hat{1}+\hat{a})(\hat{1}+\hat{b}))/2 = (\hat{1}+\hat{a}+\hat{b}+\hat{a}\hat{b})/2$. We readily get $\hat{P}$ from Eqs. (27),(28) and (29):

$$\hat{P} = \begin{pmatrix} 3r + \kappa^2 & 3l + \varepsilon \\ 3l + \varepsilon & 3p + \kappa^2 \end{pmatrix}. \tag{36}$$

Finally, the spectrum of the surface phonons is determined by the equation

$$\det \hat{P} = (3r + \kappa^2)(3p + \kappa^2) - (3l + \varepsilon)^2 = 0. \tag{37}$$

Eq. (37) reproduces the spectrum calculated before for the two limiting cases $\kappa \to 0$ and $\kappa \to \infty$ in section III. Indeed, at $\kappa \to 0$ the spectrum is $\varepsilon = \sqrt{2}\kappa + \mathcal{O}(\kappa^5)$ so that the κ^3 term is missing, while the bulk phonon starts with higher energy as $\varepsilon_B = \sqrt{2}\kappa + \kappa^3/(2\sqrt{2}) + \mathcal{O}(\kappa^5)$. Let us define the binding energy as $\delta\varepsilon = \varepsilon_B - \varepsilon$. Then the latter starts as $\kappa^3/(2\sqrt{2})$ [see Fig. 2 (c)]. Now let us consider the other limit $\kappa \to \infty$. It is easy to see that seeking the solution in the form $\varepsilon \asymp \kappa^2 + 1 - \Delta$ leads to $r = p \asymp \kappa/2 + \sqrt{2\Delta}/4$ and $l \asymp \kappa/2 - \sqrt{2\Delta}/4$ which after substitution into Eq. (37) give $2\Delta + 3\sqrt{2\Delta} - 2 = 0$. This has the same root as found before from Eq. (21), $\sqrt{2\Delta} = (\sqrt{17} - 3)/2 = \alpha_\infty \simeq 0.562$ and therefore $\delta\varepsilon_\infty = \Delta = \alpha_\infty^2/2 \simeq 0.158$.

The coincidence with the exact asymptotic results obtained in section III confirms the correctness of Eq. (37). Note that the slower decay exponent α_2 can be approximated by a simple expression $\alpha_2 = \kappa^2/(1+\kappa^2/\alpha_\infty)$ that fits the exact expression of Eq. (30) with ε from the exact solution of Eq. (37) within 0.2%. We plot the decay exponential in Fig. 2(d).

Finally, it is interesting to note that the first order approximation in powers of $z = 1/2$ in the case of the hard wall boundary conditions for surface phonons can be represented by the equation

$$\left(\hat{1} + \frac{\hat{U}_1}{2}\right)_{0,0}\left(\hat{1} + \frac{\hat{U}_1}{2}\right)_{1,1} - \left(\hat{1} + \frac{\hat{U}_1}{2}\right)_{0,1}\left(\hat{1} + \frac{\hat{U}_1}{2}\right)_{1,0} = 0 \tag{38}$$

which, distinct from the case of ripplons discussed below, *accidentally* gives the exact spectrum of Eq. (37).

B. Ripplons

Now consider the case of mixed boundary conditions for ripplons. Let us first rephrase the general form of the solution (32) in the explicit form of a vector function.
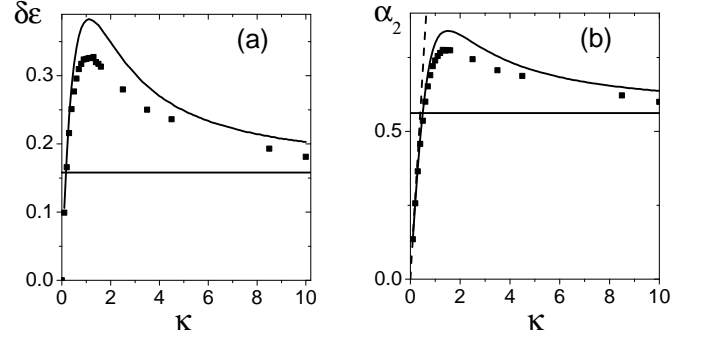

FIG. 3. *Ripplon:* (a) Dimensionless binding energy vs the dimensionless wavenumber. The squares show the results of the numerical solution of Eqs. (2) and (3) with mixed boundary conditions. The solid line is the result of the first approximation of the exact solution given by Eq. (42). The horizontal line is at energy $\Delta = 0.158$. (b) The squares show the decay parameter α_2 obtained with Eq. (30). The solid line is again the result of the first approximation of the exact solution given by Eq. (42). The horizontal line is at $\alpha_\infty = 0.568$. The analytical relation $\alpha \simeq \sqrt{2}\kappa$ at small κ is shown by the dashed line.

With the help of (34), we get

$$\begin{pmatrix} \phi_1 \\ \phi_2 \end{pmatrix} = \begin{pmatrix} A \\ B \end{pmatrix} {}_2F_1(a,b,c,z), \tag{39}$$

where A and B are arbitrary constants.

After writing the boundary conditions explicitly

$$\phi_1 = A[{}_2F_1(a,b,c,z)']_{0.0} + B[{}_2F_1(a,b,c,z)']_{0.1} = 0,$$
$$\phi_2 = A[{}_2F_1(a,b,c,z)]_{1.0} + B[{}_2F_1(a,b,c,z)]_{1.1} = 0, \tag{40}$$

the spectrum is obtained after equating the determinant of Eq. (40) to zero at $z = 1/2$. We thus proceed analogously as for the hard wall, except that in (34) there was no differentiation with respect to z in ϕ_1, so that we equated to zero the determinant of the hypergeometric function itself. Here, we separated the matrix components with primes, leading to an approximation of the exact solution in powers of $z = 1/2$ expanding the hypergeometric function of Eq. (32) and its z-derivative.

Expanding to first order in $z = 1/2$, one then gets from Eq. (40)

$$\left(\hat{U}_1 + \frac{\hat{U}_2}{2}\right)_{0,0}\left(\hat{1} + \frac{\hat{U}_1}{2}\right)_{1,1} - \left(\hat{U}_1 + \frac{\hat{U}_2}{2}\right)_{0,1}\left(\hat{1} + \frac{\hat{U}_1}{2}\right)_{1,0} = 0, \tag{41}$$

where $\hat{U}_1$ and $\hat{U}_2$ are calculated according to Eq. (33) for $m = 0, 1$ with $\hat{\alpha}$ and $\hat{a}\hat{b}$ taken from Eqs. (29) and (28),

respectively:

$$\hat{U}_2 = (\hat{\alpha} + 2\hat{1})^{-1}(\hat{a}\hat{b} + 2(\hat{\alpha} + \hat{1}))U_1$$
$$\hat{U}_1 = (\hat{\alpha} + \hat{1})^{-1}\hat{a}\hat{b}. \qquad (42)$$

C. Comparison to numerics

The energy spectrum and binding energy–decay parameter for ripplons are shown in Figs. 3 (a),(b), respectively, in comparison to their values obtained with numerical solutions of the differential equations Eqs. (2) and (3), represented by the symbols. For the numerics, we used PTC's MathCad 11, applying proper boundary conditions at the surface, *imposing* an exponentially fast decay at infinity (the latter leads to underestimate the binding energy values, see for a discussion below). One can see that even to lowest nontrivial order in the series on $z = 1/2$ [see Eq. (41)], the results shown by solid lines in Fig. 3 (a),(b) are rather close to the numerical solutions.

On the other hand, for the surface phonon, the numerical results can be rendered closer to the exact spectrum from (37), as displayed in Figs. 2 (a),(b), although a slight systematic deviation is still noticeable. These deviations stem from the fact that the numerical solution of the differential equations relies on the criterium of localization: the solution should decay into the bulk, implying that another boundary condition is that the wavefunction should approach zero at infinity. Numerical calculations are imposing boundary conditions at a finite distance, however large. The numerics therefore slightly exaggerates the decay; hence the numerical energy is slightly lower than the exact energy at a given wavenumber.

V. DISCUSSION AND CONCLUSION

We now discuss the relation of the analytically obtained binding energy of surface phonons to the experimental finding of[24] for superfluid helium confined by the hard walls of cylindrical pores. Although the present BEC model with contact interactions does not reproduce the roton minimum in the bulk dispersion curve, it gives a correct estimate for the binding energy in the low-density surface region. Indeed, the experimental binding energy, which is the difference between the bulk and the surface excitation energies for a given wavenumber, in the roton region of $k = 2\,\text{Å}^{-1}$ (using the estimate $\xi = \hbar/(mc) = 0.7\text{Å}$, with the corresponding dimensionless $\kappa = 0.96$) is 0.15 meV which corresponds to 1.8 K.

Fig. 2 (a) shows the dimensionless binding energy value of 0.07 at $\kappa = 0.96$, which corresponds to 1.77 K, and is hence rather close to the experimental value. This agreement, obtained at small wavelengths, to which previous approaches did not apply, and which in the bulk correspond to the roton minimum, indicates that, although the real bulk dispersion curve is not accurately be described by a mean-field model, the quantum mechanism of trapping the excitations near a surface has the dominant influence in determining the correct magnitude of the binding energy. We note that this quantum mechanism of binding surface excitations occurs in the solid-state physics of electrons as well, where the bound states are called Tamm and Shockley states.[32,33]

In conclusion, we have found the spectrum and wavefunctions of localized Bogoliubov elementary excitations existing near the inhomogeneous stationary solution of the Gross-Pitaevskii equation. While exact analytic solutions were previously found for both phonon and ripplon at large wavelengths,[18,22] we obtained here a complete analytical solution expressed in the form of a matrix version of Gauss' hypergeometric function. This allowed us to derive a closed algebraic expression for the whole surface-phonon spectrum. We have furthermore shown that for ripplons, even a lowest nontrivial order truncation of the hypergeometric series produces results close to numerical solutions of the BdGE. Surface modes – ripplons and surface phonons – contribute to thermodynamics of a quantum liquid at low temperatures, and the presently obtained surface-phonon branch predicts a binding energy for surface excitations in helium II confined in hard-walled pores which is close to the experimental value.[24]

The present method for exactly solving the Bogoliubov-de Gennes equations is potentially also useful in more sophisticated cases than the presently considered one. Further extensions of the present approach are conceivable also by incorporating effectively nonlocal interactions modelling rotons, which occur in dilute quantum gases dominated by dipole-dipole interactions.[34]

[1] E. P. Gross, "Structure of a quantized vortex in boson systems," Il Nuovo Cimento (1955-1965) **20**, 454 (1961).

[2] L. P. Pitaevskii, "Vortex lines in an imperfect Bose gas," Sov. Phys. JETP **13**, 451 (1961).

[3] L. Pitaevskii and S. Stringari, *Bose Einstein Condensation* (Oxford Univ. Press, NY, New York, 2003).

[4] Iacopo Carusotto and Cristiano Ciuti, "Quantum fluids of light," Rev. Mod. Phys. **85**, 299 (2013).

[5] V. E. Zakharov, "Stability of periodic waves of finite amplitude on the surface of a deep fluid," Journal of Applied Mechanics and Technical Physics **9**, 190 (1968).

[6] N. N. Bogoliubov, "On the theory of superfluidity," J. Phys.(USSR) **11**, 23 (1947).

[7] N. N. Bogoliubov, "On a new method in the theory of superconductivity," Il Nuovo Cimento **7**, 794 (1958).

[8] J. G. Valatin, "Comments on the theory of superconductivity," Il Nuovo Cimento **7**, 843 (1958).

[9] P. G. de Gennes and D. Saint-James, "Elementary excitations in the vicinity of a normal metal-superconducting metal contact," Physics Letters **4**, 151 (1963).

[10] Anthony J. Leggett, "Bose-Einstein condensation in the alkali gases: Some fundamental concepts," Rev. Mod. Phys. **73**, 307–356 (2001).

[11] Yasunari Kurita, Michikazu Kobayashi, Takao Morinari, Makoto Tsubota, and Hideki Ishihara, "Spacetime analog of Bose-Einstein condensates: Bogoliubov–de Gennes formulation," Phys. Rev. A **79**, 043616 (2009).

[12] M. Z. Hasan and C. L. Kane, "Colloquium: Topological insulators," Rev. Mod. Phys. **82**, 3045–3067 (2010).

[13] Ali Shams, J. L. DuBois, and H. R. Glyde, "Localization of Bose–Einstein Condensation by Disorder," Journal of Low Temperature Physics **145**, 357 (2006).

[14] A. Griffin and S. Stringari, "Surface region of superfluid helium as an inhomogeneous Bose-condensed gas," Phys. Rev. Lett. **76**, 259 (1996).

[15] J. R. Anglin, "Local vortex generation and the surface mode spectrum of large Bose-Einstein condensates," Phys. Rev. Lett. **87**, 240401 (2001).

[16] E. A. Kuznetsov and S. K. Turitsyn, "Instability and collapse of solitons in media with a defocusing nonlinearity," Sov. Phys. JETP. **67**, 1583 (1988).

[17] Alexander L. Gaunt, Tobias F. Schmidutz, Igor Gotlibovych, Robert P. Smith, and Zoran Hadzibabic, "Bose-Einstein Condensation of Atoms in a Uniform Potential," Phys. Rev. Lett. **110**, 200406 (2013).

[18] P. V. Pikhitsa, "Surface excitations of a nonideal bose gas," Physica B: Condensed Matter **179**, 201 (1992).

[19] L. S. Reut and I. Z. Fisher, "Surface excitations in liquid He^4," Sov. Phys. JETP. **33**, 981 (1971).

[20] Xiang-Jun Chen, Zhi-De Chen, and Nian-Ning Huang, "A direct perturbation theory for dark solitons based on a complete set of the squared Jost solutions," Journal of Physics A: Mathematical and General **31**, 6929 (1998).

[21] A. E. Muryshev, H. B. van Linden van den Heuvell, and G. V. Shlyapnikov, "Stability of standing matter waves in a trap," Phys. Rev. A **60**, R2665 (1999).

[22] Daisuke A. Takahashi, Michikazu Kobayashi, and Muneto Nitta, "Nambu-Goldstone modes propagating along topological defects: Kelvin and ripple modes from small to large systems," Phys. Rev. B **91**, 184501 (2015).

[23] S. O. Diallo, R. T. Azuah, D. L. Abernathy, Junko Taniguchi, Masaru Suzuki, Jacques Bossy, N. Mulders, and H. R. Glyde, "Evidence for a Common Physical Origin of the Landau and BEC Theories of Superfluidity," Phys. Rev. Lett. **113**, 215302 (2014).

[24] Timothy R. Prisk, Narayan C. Das, Souleymane O. Diallo, Georg Ehlers, Andrey A. Podlesnyak, Nobuo Wada, Shinji Inagaki, and Paul E. Sokol, "Phases of superfluid helium in smooth cylindrical pores," Phys. Rev. B **88**, 014521 (2013).

[25] V. L. Ginzburg and L. P. Pitaevskii, "On the theory of superfluidity," Soviet Physics JETP **7**, 858 (1958).

[26] J. Dziarmaga, "Quantum dark soliton: Nonperturbative diffusion of phase and position," Phys. Rev. A **70**, 063616 (2004).

[27] The snake instability amounts to a *moving* wall (a nodal plane) with its transverse parts moving at different velocities, which is hence acting to destroy the wall.

[28] L. D. Landau and E. M. Lifshitz, *Quantum Mechanics* (Pergamon Press, New York, 1977) [p. 73, problem 5].

[29] By making use of the known solutions of the homogeneous equations (10) and (11), to satisfy the boundary conditions.

[30] Juan A. Tirao, "The matrix-valued hypergeometric equation," Proceedings of the National Academy of Sciences **100**, 8138 (2003).

[31] L Jódar and J.C Cortés, "Some properties of Gamma and Beta matrix functions," Applied Mathematics Letters **11**, 89 (1998).

[32] I. E. Tamm, "On the possible bound states of electrons on a crystal surface," Phys. Z. Sowjetunion. **1**, 733 (1932).

[33] William Shockley, "On the Surface States Associated with a Periodic Potential," Phys. Rev. **56**, 317 (1939).

[34] Uwe R. Fischer, "Stability of quasi-two-dimensional Bose-Einstein condensates with dominant dipole-dipole interactions," Phys. Rev. A **73**, 031602 (2006).